

# **Hydrogen Production by Water Dissociation using Ceramic Membranes**

---

*Annual Report for FY 2008*

**Energy Systems Division**

**About Argonne National Laboratory**

Argonne is a U.S. Department of Energy laboratory managed by UChicago Argonne, LLC under contract DE-AC02-06CH11357. The Laboratory's main facility is outside Chicago, at 9700 South Cass Avenue, Argonne, Illinois 60439. For information about Argonne and its pioneering science and technology programs, see [www.anl.gov](http://www.anl.gov).

**Availability of This Report**

This report is available, at no cost, at <http://www.osti.gov/bridge>. It is also available on paper to the U.S. Department of Energy and its contractors, for a processing fee, from:

U.S. Department of Energy  
Office of Scientific and Technical Information  
P.O. Box 62  
Oak Ridge, TN 37831-0062  
phone (865) 576-8401  
fax (865) 576-5728  
[reports@adonis.osti.gov](mailto:reports@adonis.osti.gov)

**Disclaimer**

This report was prepared as an account of work sponsored by an agency of the United States Government. Neither the United States Government nor any agency thereof, nor UChicago Argonne, LLC, nor any of their employees or officers, makes any warranty, express or implied, or assumes any legal liability or responsibility for the accuracy, completeness, or usefulness of any information, apparatus, product, or process disclosed, or represents that its use would not infringe privately owned rights. Reference herein to any specific commercial product, process, or service by trade name, trademark, manufacturer, or otherwise, does not necessarily constitute or imply its endorsement, recommendation, or favoring by the United States Government or any agency thereof. The views and opinions of document authors expressed herein do not necessarily state or reflect those of the United States Government or any agency thereof, Argonne National Laboratory, or UChicago Argonne, LLC.

## **Hydrogen Production by Water Dissociation using Ceramic Membranes**

---

*Annual Report for FY 2008*

by  
U. (Balu) Balachandran, S.E. Dorris, J.E. Emerson, T.H. Lee, Y. Lu, C.Y. Park, and J.J. Picciolo  
Energy Systems Division, Argonne National Laboratory

February 11, 2009

**HYDROGEN PRODUCTION BY WATER DISSOCIATION  
USING CERAMIC MEMBRANES**

**ANNUAL REPORT FOR FY 2008**

ARGONNE NATIONAL LABORATORY

Energy Systems Division

9700 South Cass Avenue

Argonne, Illinois 60439

U. (Balu) Balachandran

*Contributors:*

S. E. Dorris

Y. Lu

J. E. Emerson

C.Y. Park

T. H. Lee

J. J. Picciolo

February 11, 2009

Work Supported by

U. S. DEPARTMENT OF ENERGY

Office of Fossil Energy, National Energy Technology Laboratory

Argonne National Laboratory is a U.S. Department of Energy laboratory managed by UChicago Argonne, LLC, under Contract Number DE-AC-02-06CH11357.

## Contents

---

I. Objective.....	1
II. Highlights.....	1
III. Introduction.....	2
IV. Results.....	3
Milestone 1: Continue to develop new membrane materials .....	3
Milestone 2: Fabricate and test tubular membranes for hydrogen production .....	13
Milestone 3: Test concept of using coal combustion to drive water dissociation for hydrogen production.....	20
Milestone 4: Evaluate chemical stability of the membranes .....	22
V. Future Work.....	24
Publications and Presentations.....	26
References.....	27

## Figures

---

1. Secondary electron images of SFC2 film sintered in Ar for 7 h at 1160°C and annealed for 5 h at 750°C: (a) fracture surface after hydrogen production rate measurements and (b) as-sintered surface.....	4
2. As-sintered surfaces of SFC2 films sintered in (a) 200 ppm H <sub>2</sub> /balance N <sub>2</sub> and (b) air .....	5
3. Hydrogen production rate vs. pH <sub>2</sub> O on hydrogen-generation side of SFC2 tested at 900°C using 80% H <sub>2</sub> /balance He on oxygen-permeate side .....	6
4. Hydrogen production rate at 900°C vs. pH <sub>2</sub> O on hydrogen-generation side of SFC2 film on carbon-containing substrate and tested using 80% H <sub>2</sub> /balance He on oxygen-permeate side.....	6
5. Hydrogen production rate vs. pH <sub>2</sub> O on hydrogen-generation side of LSCF7328 at 900°C using 80% H <sub>2</sub> /balance He on oxygen-permeate side.....	7
6. Hydrogen production rate of LSCF7328 vs. inverse of membrane thickness at 900°C with 80% H <sub>2</sub> /balance He on oxygen-permeate side and pH <sub>2</sub> O = 0.49 atm on hydrogen-generation side. ....	8
7. Hydrogen production rate of LSCF7328 vs. inverse temperature with pH <sub>2</sub> O = 0.49 atm on hydrogen-generation side and 80% H <sub>2</sub> /balance He on oxygen-permeate side .....	8
8. Hydrogen production rate vs. inverse of thickness for LSCF7328 disks with and without porous Pt coating, measured at 900°C with 80% H <sub>2</sub> /balance He on oxygen-permeate side and humidified nitrogen on hydrogen-generation side. ....	9
9. Hydrogen production rate vs. pH <sub>2</sub> O at 900°C for LSCF7328 thin films on porous LSCF7328 substrates made with 20% carbon and dense LSCF7328 substrate made without carbon .....	11
10. SEM micrographs of SFT1 and SdFT1 disk-type thin films.....	12
11. Spring-loaded fixture for measuring hydrogen production rate.....	13
12. Hydrogen production rate at 900°C vs. pH <sub>2</sub> O on hydrogen-generation side of SFC2 tube with 80% H <sub>2</sub> /He on oxygen-permeate side .....	14
13. Hydrogen production rate of SFC2 tube vs. inverse temperature using humidified N <sub>2</sub> on hydrogen-generation side and 80% H <sub>2</sub> /balance He on oxygen-permeate side.....	15

14. Hydrogen production rates vs. $p_{H_2O}$ on hydrogen-generation side of SFC2 tube at 900°C using 80% $H_2/He$ , CO, and 25% CO/75% $CO_2$ on oxygen-permeate side.....	16
15. Thin-film SFC2 tube made by paste-painting technique: a) photograph, b) "low" magnification cross-sectional view, and c) "high" magnification cross-sectional view .....	17
16. Hydrogen production rate vs. temperature for thin-film and self-supported SFC2 tubes, measured with 80% $H_2/balance\ He$ on oxygen-permeate side and humidified $N_2$ on steam side.....	17
17. Hydrogen production rate vs. $p_{H_2O}$ on steam side of thin-film and self-supported SFC2 tube, measured at 900°C with 80% $H_2/He$ on oxygen-permeate side .....	18
18. Hydrogen production rate of thin-film SFC2 tube vs. flow rate of humidified $N_2$ on steam side of tube.....	19
19. Hydrogen production rate of $\approx 22\text{-}\mu\text{m}$ -thick LSCF7328 thin film on porous LSCF7328 substrate made with 20% C vs. temperature and CO concentration in gas on oxygen-permeate side with balance of He or $CO_2$ .....	21
20. Hydrogen production rate of $\approx 22\text{-}\mu\text{m}$ -thick LSCF7328 thin film on porous LSCF7328 substrate made with 20% C vs. inverse temperature using various CO/ $CO_2$ gas mixtures on oxygen-permeate side of film. ....	22
21. Hydrogen production rate at 900°C for SFC2 tube during test of its chemical stability .....	24

## Tables

---

1. Effect of gas flow rates on hydrogen production rate of tubular SFC2 thin film.....	19
2. Composition of atmosphere on oxygen-permeate side of SFC2 tube during test of tube's chemical stability at 900°C.....	23

**HYDROGEN PRODUCTION BY WATER DISSOCIATION  
USING CERAMIC MEMBRANES**

**ANNUAL REPORT FOR FY 2008**

**ARGONNE NATIONAL LABORATORY**

Project Title: Hydrogen Production by Water Dissociation using Ceramic Membranes

NETL Project Manager: Richard Dunst

ANL Project PI: U. (Balu) Balachandran

B&R Code/Contract Number: AA-10-40-00-00-0/FWP 49347

Report Date: February 11, 2009

**I. OBJECTIVE**

The objective of this project is to develop dense ceramic membranes that, without using an external power supply or circuitry, can produce hydrogen via coal/coal gas-assisted water dissociation.

**II. HIGHLIGHTS**

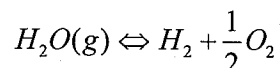
1. A  $\text{SrFeCo}_{0.5}\text{O}_x$  (SFC2) thin film made by a modified sintering procedure gave the highest hydrogen production rate to date for an Argonne membrane,  $17.4 \text{ cm}^3/\text{min}\text{-cm}^2$ .
2. Materials in the La-Sr-Cu-Fe-oxide system were tested as oxygen transport membranes (OTMs) for use at low temperature ( $\leq 700^\circ\text{C}$ ). The hydrogen production rate of  $\text{La}_{0.7}\text{Sr}_{0.3}\text{Cu}_{0.2}\text{Fe}_{0.8}\text{O}_{3-\delta}$  (LSCF7328) thin films was measured at  $600\text{-}900^\circ\text{C}$ .
3. Methods were developed to fabricate self-supporting and thin-film tubular OTMs.
4. The hydrogen production rates of self-supporting and thin-film SFC2 tubes were measured as a function of temperature in the range  $500\text{-}900^\circ\text{C}$ .
5. The hydrogen production rate of an OTM was measured by using  $\text{CO}/\text{CO}_2$  gas mixtures to drive water dissociation.
6. An SFC2 tube was found to be stable during  $>700$  h of testing at  $900^\circ\text{C}$  with various  $\text{CO}/\text{CO}_2$  mixtures on the oxygen-permeate side of the tube and  $\text{N}_2$  ( $0.03 \text{ atm H}_2\text{O}$ ) on the hydrogen-generation side.

### III. INTRODUCTION

This project grew from an effort to develop a dense ceramic membrane for separating hydrogen from gas mixtures such as those generated during coal gasification, methane partial oxidation, and water-gas shift reactions [1]. That effort led to the development of various cermet (i.e., ceramic/metal composite) membranes that enable hydrogen production by two methods. In one method, a hydrogen transport membrane (HTM) selectively removes hydrogen from a gas mixture by transporting it through either a mixed protonic/electronic conductor or a hydrogen transport metal. In the other method, an oxygen transport membrane (OTM) generates hydrogen mixed with steam by removing oxygen that is generated through water splitting [1, 2].

This project focuses on the development of OTMs that efficiently produce hydrogen via the dissociation of water. Supercritical boilers offer very high-pressure steam that can be decomposed to provide pure hydrogen by means of OTMs. Oxygen resulting from the dissociation of steam can be used for coal gasification, enriched combustion, or synthesis gas production. Hydrogen and sequestration-ready CO<sub>2</sub> can be produced from coal and steam by using the membrane being developed in this project. Although hydrogen can also be generated by high-temperature steam electrolysis, producing hydrogen by water splitting with a mixed-conducting membrane requires no electric power or electrical circuitry.

Water dissociates into oxygen and hydrogen at high temperatures by the reaction:



However, very low concentrations of hydrogen and oxygen are generated even at relatively high temperatures (e.g., 0.1 and 0.042% for hydrogen and oxygen, respectively, at 1600°C), because the equilibrium constant for the reaction is small [3]. This shortcoming can be overcome at moderate temperatures by using a mixed-conducting (electron- and ion-conducting) membrane to remove either oxygen or hydrogen, which shifts the equilibrium toward dissociation. If an OTM is used to produce hydrogen, the hydrogen production rate depends directly on the rate at which oxygen is removed from the water dissociation zone, which depends on the OTM's oxygen permeability (a function of the OTM's electron and oxygen-ion conductivities), the surface oxygen exchange kinetics, and the oxygen partial pressure (pO<sub>2</sub>) gradient across the OTM [4-7]. To obtain a high hydrogen production rate, mixed-conducting OTMs should exhibit high electron and oxygen-ion conductivities, should possess good surface exchange properties, and should be exposed to a high pO<sub>2</sub> gradient.

Others have used mixed-conducting OTMs to produce hydrogen by water dissociation, but the membranes had low electronic conductivity, and the hydrogen production rate was modest even at high temperature (e.g., 0.6 cm<sup>3</sup> (STP)/min-cm<sup>2</sup> at 1683°C [8]). We achieved a significantly higher hydrogen production rate using an OTM composed of an oxygen-ion conductor of cerium gadolinium oxide (CGO) and an electronic conductor (Ni) [2]. The hydrogen production rate increased with increases in temperature, water partial pressure on the hydrogen-production side of the membrane, and oxygen chemical potential gradient across the membrane [2]. It also increased with decreasing membrane thickness, but it became limited by surface reaction kinetics for OTMs with thickness < ≈0.5 mm.

To be practical for hydrogen production, OTMs must give high hydrogen production rates and be available in a shape with a large active area, e.g., tubes. The OTMs must also remain chemically and mechanically stable in corrosive environments at elevated temperatures. This report summarizes progress during FY 2008 toward the fabrication of practical OTMs. As benchmarks in the development of practical OTMs, the following milestones were established in the Field Work Proposal for FY 2008:

1. Continue to develop new membrane materials.
2. Fabricate and test tubular membranes for hydrogen production.
3. Test concept of using coal combustion to drive water dissociation for hydrogen production.
4. Evaluate chemical stability of the membranes.

All experimental milestones for FY 2008 were met in tests using OTMs that were developed at Argonne. In addition, we continued developing new membrane materials and fabrication methods to enhance the hydrogen production rate of OTMs.

#### IV. RESULTS

Results obtained during FY 2008 are presented below in relation to the pertinent milestone.

##### **Milestone 1. Continue to develop new membrane materials.**

High hydrogen production rates can be achieved with an OTM composed of SrFeCo<sub>0.5</sub>O<sub>x</sub> (SFC2); however, the atmosphere for sintering strongly influences the properties of SFC2 thin films on porous SFC2 substrates. An SFC2 film (thickness  $\approx 30$   $\mu\text{m}$ ) sintered in air gave a hydrogen production rate of  $\approx 6.5$   $\text{cm}^3/\text{min}\cdot\text{cm}^2$ , whereas a significantly thicker pressed SFC2 disk (thickness  $\approx 210$   $\mu\text{m}$ ) gave a rate of  $\approx 7.5$   $\text{cm}^3/\text{min}\cdot\text{cm}^2$  after it was sintered in 200 ppm H<sub>2</sub>/balance N<sub>2</sub>. The SFC2 samples sintered in ambient air had large ( $>5$ - $10$   $\mu\text{m}$ ) plate-like crystals, whereas samples sintered in 200 ppm H<sub>2</sub>/N<sub>2</sub> had small (1-2  $\mu\text{m}$ ) equiaxed grains. Combining the microstructural observations with the hydrogen production rates suggested that a finer, equiaxed microstructure was more conducive to a high hydrogen production rate; unfortunately, SFC2 thin films sintered in 200 ppm H<sub>2</sub> tended to crack and/or warp during sintering. Modifications to the sintering process enabled the fabrication of SFC2 thin films in oxygen-free atmospheres. An SFC2 thin film made with these modifications gave the highest hydrogen production rate to date for an Argonne OTM, 17.4  $\text{cm}^3/\text{min}\cdot\text{cm}^2$ .

Next, SFC2 thin films were fabricated on porous SFC2 substrates for mechanical support. Porous SFC2 substrates were prepared by blending a binder with a homogeneous mixture of SFC2 (Praxair Specialty Ceramics) and carbon (20 or 30 wt.%, Fisher Scientific) powders. The mixture of SFC2, carbon, and binder was milled in isopropyl alcohol (IPA) for 24 h, and then the alcohol was evaporated. Dried powder was passed through a 120-mesh sieve and was uniaxially pressed (29,000 psi) into disks ( $\approx 2$ -mm thick x 22-mm dia.) that were pre-sintered for 5 h in air at 950-1000°C to remove the carbon and provide the disks with mechanical integrity.

To fabricate dense SFC2 thin films, a colloidal suspension was prepared from SFC2 powder with an average particle size of  $\approx 0.9 \mu\text{m}$ . The SFC2 powder and an organic dispersant were mixed in IPA for 30 min in an ultrasonic bath to break up agglomerates and disperse the powders. To deposit a thin film, the colloidal suspension was cast onto a pre-sintered SFC2 substrate. The green film and substrate were then sintered in an atmosphere of flowing argon, 200 ppm  $\text{H}_2$ /balance  $\text{N}_2$ , or ambient air. After sintering, films were annealed for 5 h at  $750^\circ\text{C}$  in the same atmosphere that was used for sintering. Sufficient porosity was retained in substrates during sintering by incorporating carbon powder (20 or 30 wt.%) as a pore former.

We sealed a membrane to the end of an  $\text{Al}_2\text{O}_3$  tube using a gold gasket and a spring-loaded assembly described elsewhere [9]. During measurement of the hydrogen production rate, nitrogen was bubbled through water at a fixed temperature to control the steam partial pressure ( $p_{\text{H}_2\text{O}}$ ), and then was flowed over one side of the membrane, defined as the hydrogen-generation side. The temperature of the water bath was adjusted to control  $p_{\text{H}_2\text{O}}$ . Gas containing 4-80%  $\text{H}_2$ /balance helium was flowed over the other side of the membrane, called the oxygen-permeate side. Hydrogen-helium mixtures were prepared by mixing ultrahigh-purity (UHP) hydrogen and UHP helium with mass flow controllers. Using a Hewlett-Packard 6890 gas chromatograph to measure hydrogen concentrations, we determined the hydrogen production rate at temperatures of  $500\text{-}900^\circ\text{C}$ .

Sintering SFC2 thin films in an oxygen-free atmosphere and annealing them at  $750^\circ\text{C}$  enabled the fabrication of flat, crack-free films with a fine, equiaxed microstructure. Figure 1 shows scanning electron microscopy (SEM) images of an  $\approx 20\text{-}\mu\text{m}$ -thick SFC2 film (Fig. 1a) that was sintered in Ar for 7 h at  $1160^\circ\text{C}$  and then annealed for 5 h at  $750^\circ\text{C}$ . The film appears dense (Fig. 1b) and has small, equiaxed grains. This microstructure is like that of samples sintered in 200 ppm  $\text{H}_2$  (Fig. 2a) and shows none of the large plate-like crystals that are found in air-sintered samples (Fig. 2b).

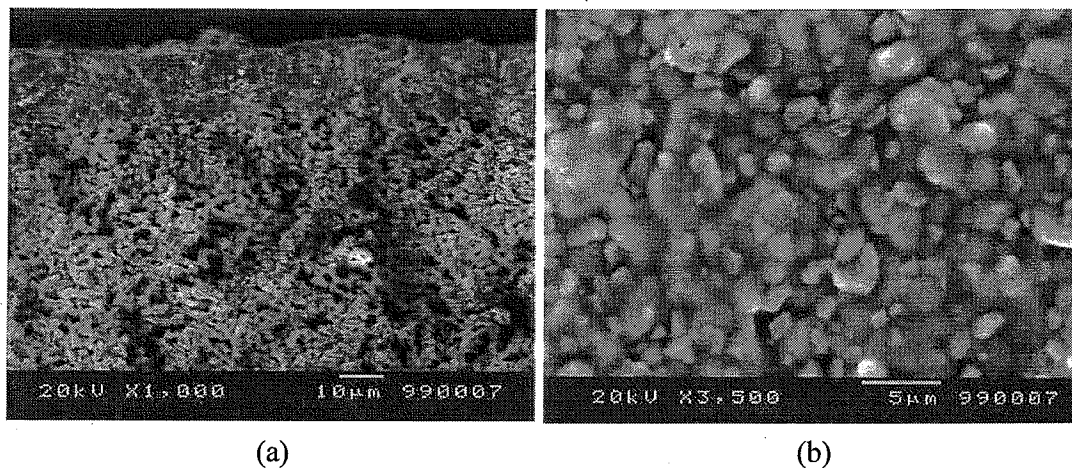


*Fig. 1 Secondary electron images of SFC2 film sintered in Ar for 7 h at  $1160^\circ\text{C}$  and annealed for 5 h at  $750^\circ\text{C}$ : (a) fracture surface after hydrogen production rate measurements and (b) as-sintered surface. Substrates were prepared from SFC2 powder with 20 wt.% carbon.*

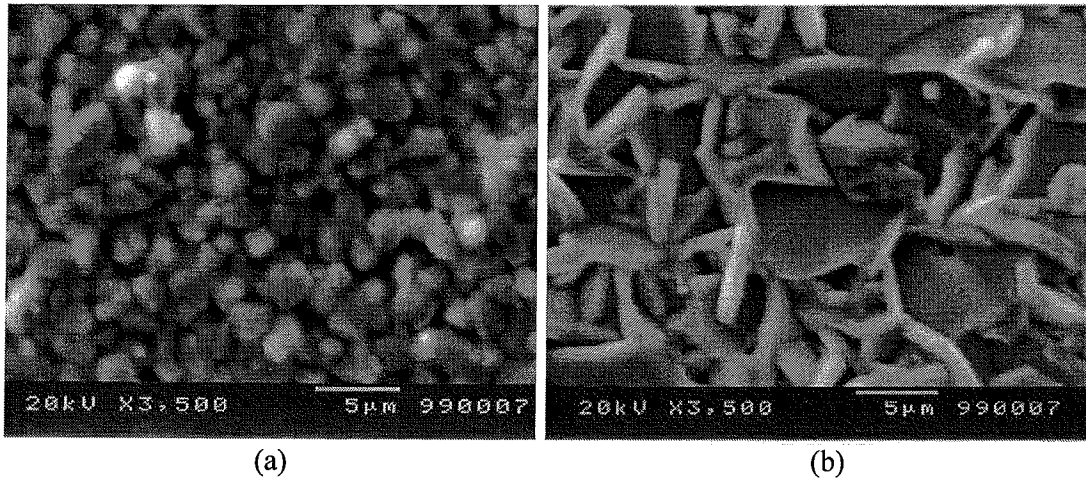


Fig. 2 As-sintered surfaces of SFC2 films sintered in (a) 200 ppm  $H_2$ /balance  $N_2$  and (b) air.

The sintering atmosphere significantly influenced the hydrogen production rate of SFC2 thin films. The hydrogen production rate was measured at  $900^\circ\text{C}$  versus  $p_{H_2O}$  on the hydrogen-generation side while dry 80%  $H_2$ /balance He was flowed on the oxygen-permeate side. Figure 3 compares the hydrogen production rate of two SFC2 films sintered in air and two films sintered in Ar, all of which were on substrates made from powder with 20 wt.% carbon. The hydrogen production rates for films sintered in Ar were similar to those of air-sintered films at low  $p_{H_2O}$  but were much higher at high  $p_{H_2O}$ . With  $p_{H_2O} = 0.49$  atm, a film sintered in Ar (thickness  $\approx 20$   $\mu\text{m}$ ) gave a hydrogen production rate of  $12.4$   $\text{cm}^3/\text{min}\cdot\text{cm}^2$ .

The hydrogen production rates of three SFC2 films are plotted in Fig. 4. Two films were made on substrates made from powder with 30 wt.% carbon; one film was sintered in Ar and the other in 200 ppm  $H_2$ /balance  $N_2$ . A third film was sintered in Ar on a substrate made with powder that contained 20 wt.% carbon. Changing the sintering atmosphere from Ar to 200 ppm  $H_2/N_2$  had little effect on the hydrogen production rate of films on substrates made with 30 wt.% carbon. Films sintered in Ar or 200 ppm  $H_2$ /balance  $N_2$  had similar surface microstructures (Figs. 1b and 2a, respectively), and both films gave a significantly higher hydrogen production rate than  $\approx 6.5$   $\text{cm}^3/\text{min}\cdot\text{cm}^2$ , the value that was obtained for an  $\approx 30$ - $\mu\text{m}$ -thick film sintered in air and tested under the same conditions. The critical factor in achieving a high hydrogen production rate appears to be that the sintering atmosphere was oxygen-free, and it seems less important whether the sintering atmosphere was 200 ppm  $H_2/N_2$  or Ar.

The carbon content of the powder used to prepare substrates affected the hydrogen production rate more significantly than did the selection of 200 ppm  $H_2/N_2$  or Ar as the sintering atmosphere. At low  $p_{H_2O}$ , the absolute difference in the hydrogen production rates was not large for the three films, but the effect of carbon content was stronger at high  $p_{H_2O}$ . Both films on substrates made with 30 wt.% carbon gave a rate of  $\approx 14.3$   $\text{cm}^3/\text{min}\cdot\text{cm}^2$  at  $p_{H_2O} = 0.49$  atm, compared to  $\approx 12.4$   $\text{cm}^3/\text{min}\cdot\text{cm}^2$  for the film made with 20 wt.% carbon. The higher carbon content should yield more porosity in the substrate after sintering, which would enhance gas transport and reduce concentration polarization. At  $p_{H_2O} = 0.69$  atm, the film sintered in 200 ppm  $H_2/N_2$  gave a hydrogen production rate of  $17.4$   $\text{cm}^3/\text{min}\cdot\text{cm}^2$ , the highest value measured to this point at Argonne.

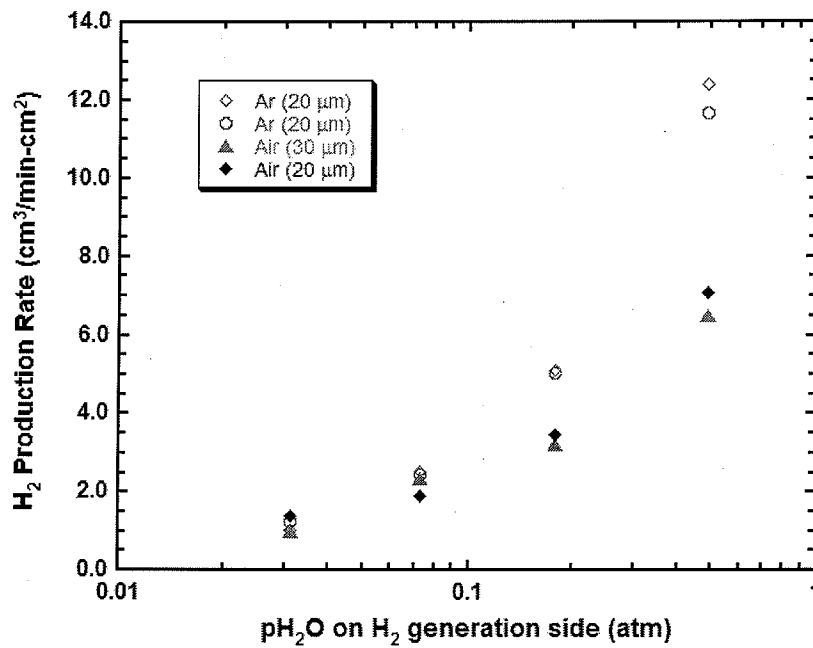


Fig. 3 Hydrogen production rate vs.  $p_{H_2O}$  on hydrogen-generation side of SFC2 at 900°C using 80%  $H_2$ /balance He on oxygen-permeate side. Inset gives atmosphere and membrane thickness.

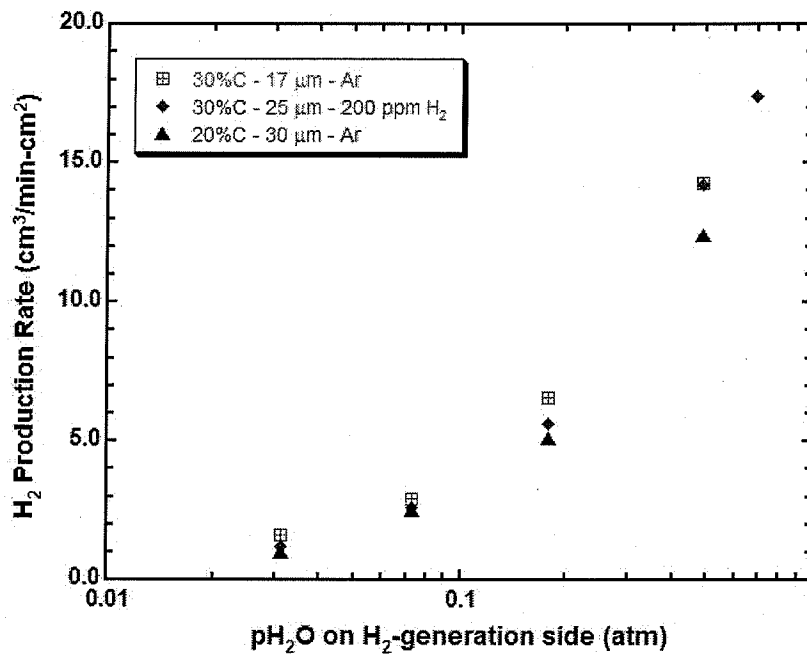


Fig. 4 Hydrogen production rate vs.  $p_{H_2O}$  on hydrogen-generation side of SFC2 film on carbon-containing substrate and tested at 900°C using 80%  $H_2$ /balance He on oxygen-permeate side. Inset gives membrane thickness and atmosphere for sintering and annealing.

Materials in the La-Sr-Cu-Fe-oxide system, which exhibit high electrocatalytic activity and were originally studied to improve the performance of cathodes for intermediate temperature solid oxide fuel cells, are being tested as OTMs. We prepared  $\text{La}_{0.7}\text{Sr}_{0.3}\text{Cu}_{0.2}\text{Fe}_{0.8}\text{O}_{3-\delta}$  (LSCF7328) by conventional solid-state synthesis using  $\text{La}_2\text{O}_3$  from Alfa Aesar (99.999%),  $\text{SrCO}_3$  from Aldrich (99.9+%),  $\text{CuO}$  from Johnson Matthey (99.999%), and  $\text{Fe}_2\text{O}_3$  from Alfa Aesar (99.99%) as the starting materials. Stoichiometric amounts of the starting materials were mixed and milled with zirconia balls in IPA for two days. The mixture was dried, calcined at  $900^\circ\text{C}$  for 5 h in air, and then ball milled with binder overnight. Dried powder was uniaxially pressed into a disk at 7,000 psi. Dense ceramic discs were obtained by sintering pressed disks in air at  $1150\text{--}1190^\circ\text{C}$  for 24 h. To measure the hydrogen production rate, both sides of a dense disc were polished with 600-grit SiC polishing paper.

The hydrogen production rates for four samples of LSCF7328 are shown as a function of  $p_{\text{H}_2\text{O}}$  on the hydrogen-generation side of the membrane (Fig. 5), inverse membrane thickness (Fig. 6), and inverse temperature (Fig. 7). Figure 5 shows the hydrogen production rate at  $900^\circ\text{C}$  versus  $p_{\text{H}_2\text{O}}$  on the hydrogen-generation side of the samples. This rate was measured while flowing 80%  $\text{H}_2$ /balance He on the oxygen-permeate side. As expected, it increased with increasing  $p_{\text{H}_2\text{O}}$  and decreasing membrane thickness due to an increase in  $p_{\text{O}_2}$  gradient across the membrane. For reference, the hydrogen production rate is shown for a CGO/Ni membrane with thickness of 0.97 mm. Neither the CGO/Ni membrane nor the LSCF7328 membranes had porous layers on their surfaces. The hydrogen production rate of CGO/Ni was higher than that of all the LSCF7328 samples, even though the thickness of some LSCF7328 samples was considerably smaller.

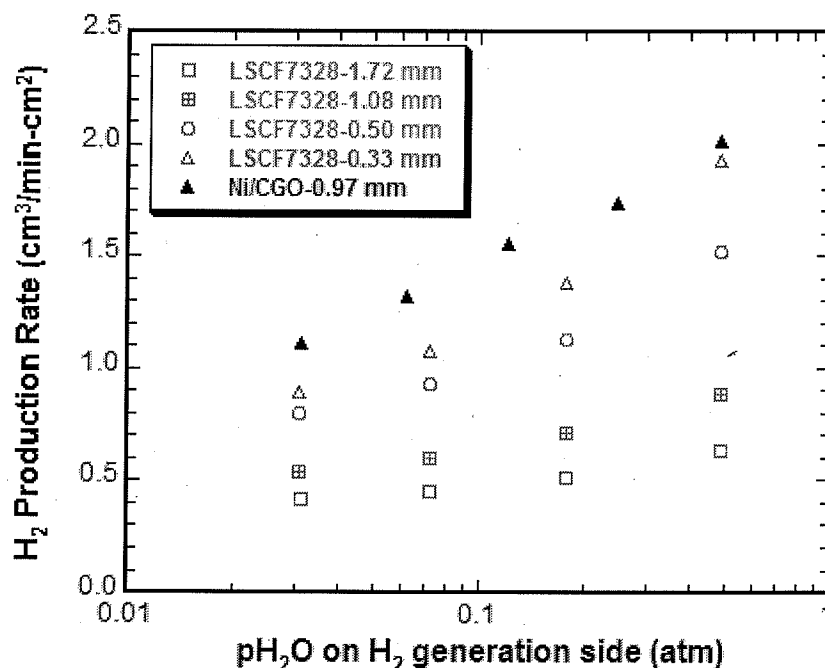


Fig. 5 Hydrogen production rate vs.  $p_{\text{H}_2\text{O}}$  on hydrogen-generation side of LSCF7328 at  $900^\circ\text{C}$  using 80%  $\text{H}_2$ /balance He on oxygen-permeate side. Inset gives membrane thickness.

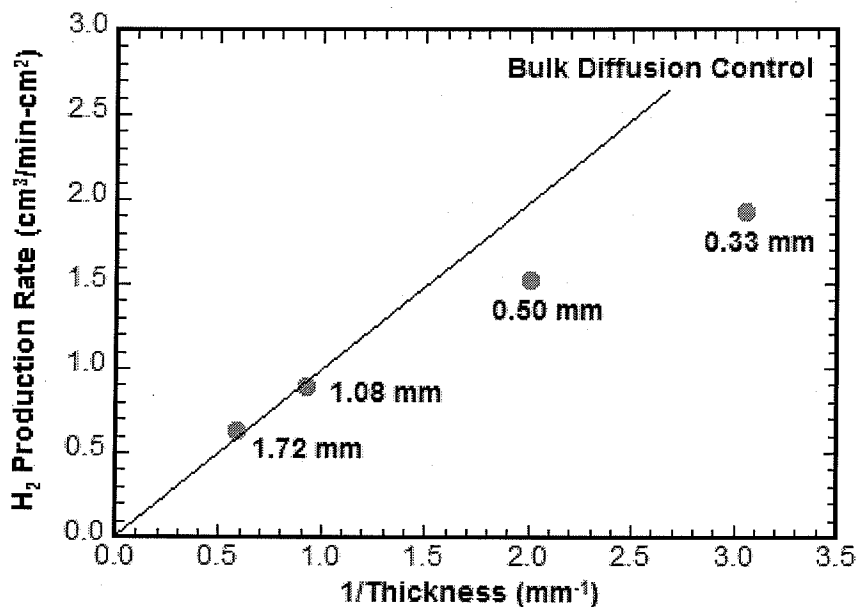


Fig. 6 Hydrogen production rate of LSCF7328 vs. inverse of membrane thickness at 900°C with 80% H<sub>2</sub>/balance He on oxygen-permeate side and p<sub>H<sub>2</sub>O</sub> = 0.49 atm on hydrogen-generation side.

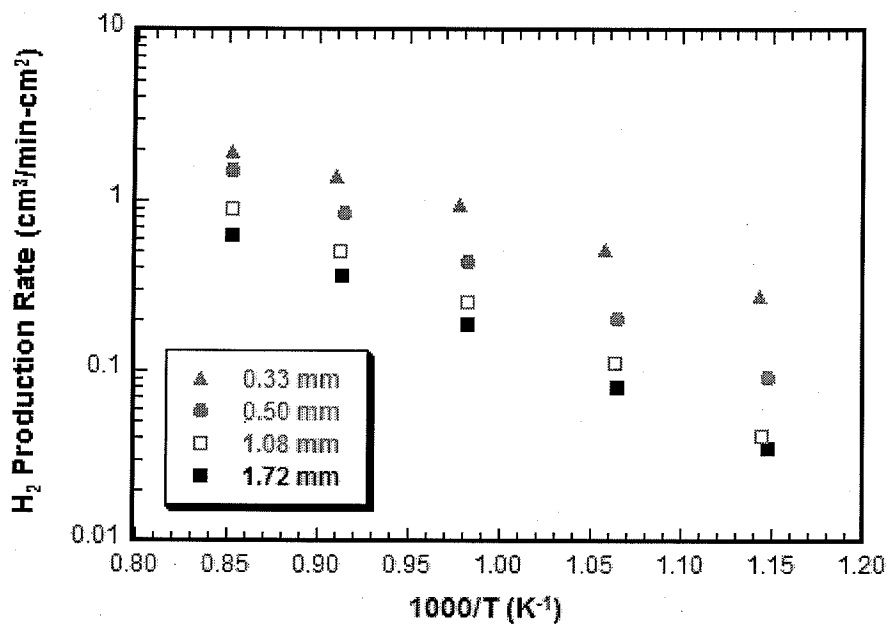


Fig. 7 Hydrogen production rate of LSCF7328 disks vs. inverse temperature with 80% H<sub>2</sub>/balance He on oxygen-permeate side, p<sub>H<sub>2</sub>O</sub> = 0.49 atm on hydrogen-generation side. Inset gives membrane thickness.

Figure 6 shows the hydrogen production rate versus the inverse thickness of the LSCF7328 membranes. For thick membranes (inverse thickness  $< 1 \text{ mm}^{-1}$ ), the hydrogen production rate appears to extrapolate through zero. In this thickness range ( $> \approx 1 \text{ mm}$ ), bulk diffusion of oxygen dominates the hydrogen production rate. The line labeled "bulk diffusion control" indicates how the hydrogen production rate would vary if it were controlled strictly by bulk diffusion without any limitations from surface reaction kinetics. For thin ( $< 1 \text{ mm}$ ) membranes, surface reaction kinetics become important, as indicated by the hydrogen production rate for these samples falling below the line for bulk diffusion control.

The hydrogen production rate versus inverse temperature (Fig. 7) was used to calculate the apparent activation energy for each membrane. The apparent activation energy varies from  $\approx 0.89 \text{ eV}$  for thick samples to  $0.56 \text{ eV}$  for the thinnest sample. Because the activation energy for surface diffusion is generally lower than that for bulk diffusion, the decrease in activation energy is consistent with the idea that surface reaction kinetics begin to dominate the behavior of thin samples.

To reduce limitations from surface reaction kinetics, we next coated thin samples of LSCF7328 with porous surface layers. Figure 8 plots the hydrogen production rate at  $900^\circ\text{C}$  versus the inverse thickness for two types of LSCF7328 membranes: disks that had no surface treatment other than polishing with 600 grit SiC paper and disks that were polished and then coated with porous Pt to enhance the surface reaction kinetics. The measurements were made while flowing humidified nitrogen ( $p_{\text{H}_2\text{O}} = 0.49 \text{ atm}$ ) over the hydrogen-generation side of the disks and  $80\% \text{ H}_2/\text{balance He}$  over the oxygen-permeate side.

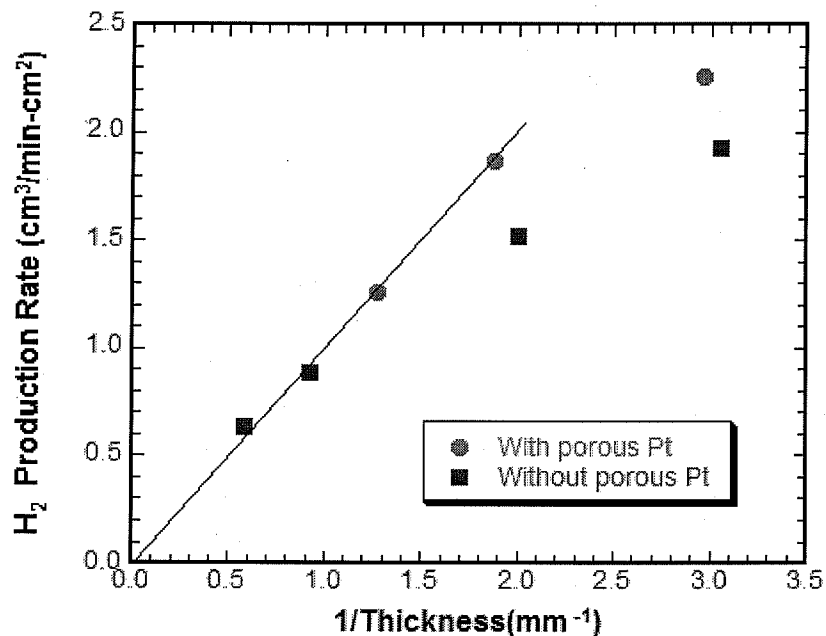


Fig. 8 Hydrogen production rate vs. inverse of thickness for LSCF7328 disks with or without porous Pt coating, measured at  $900^\circ\text{C}$  with  $80\% \text{ H}_2/\text{balance He}$  on oxygen-permeate side and humidified nitrogen ( $p_{\text{H}_2\text{O}} = 0.49 \text{ atm}$ ) on hydrogen-generation side.

The hydrogen production rate of the disk without porous Pt varies linearly with inverse membrane thickness or inverse thickness  $<1 \text{ mm}^{-1}$ , but deviates from linearity at larger values of inverse thickness. The departure from linearity indicates the thickness at which surface reaction kinetics begin to dominate the behavior of thin membranes. In comparison, membranes coated with a porous Pt layer exhibit linear behavior up to an inverse thickness of  $\approx 2 \text{ mm}^{-1}$ , and they give a higher hydrogen production rate than uncoated membranes with a similar thickness. The higher rate at a given thickness and the persistence of linear behavior to larger values of inverse thickness indicate that the porous Pt layer enhances the surface reaction kinetics.

With better surface reaction kinetics due to the porous Pt layers, reducing the membrane thickness might further increase the hydrogen production rate of LSCF7328 membranes; therefore, we measured the hydrogen production rate of Pt-coated, thin ( $<50 \text{ }\mu\text{m}$ ) films of LSCF7328 on porous LSCF7328 substrates. Porous LSCF7328 substrates were made as supports for LSCF7328 thin films, because using the same material for substrate and thin film eliminates stresses from a mismatch in the coefficient of thermal expansion. Substrates were prepared with two different densities to study the effect of porosity on the hydrogen production rate. Substrates were prepared from either LSCF7328 powder mixed with 20 wt.% carbon or LSCF7328 powder without carbon. When LSCF7328 powder was mixed with carbon, the mixture was ball-milled overnight in isopropyl alcohol, and then dried. Powders for substrates were uniaxially pressed into disks and then fired for 10 h at  $1050^\circ\text{C}$  in ambient air. After firing, the density of substrates was measured by the Archimedes method.

Thin films were prepared by painting the surface of porous LSCF7328 substrates with a slurry containing LSCF7328 powder. To prepare the slurry, LSCF7328 powder was mixed with proper amounts of a binder (polyvinyl butyral), plasticizer, and solvent ( $\alpha$ -terpineol). After the slurry was painted onto a substrate with a brush, the sample was dried for 1 h at  $80^\circ\text{C}$ , and then sintered at  $1100\text{--}1140^\circ\text{C}$  for 10 h in air. To produce a porous Pt layer on the surface of the thin film, it was painted with Pt paste and fired at  $850^\circ\text{C}$  for 30 min in air. The microstructures of samples were investigated with a JEOL JSM-5400 scanning electron microscope.

For measurement of the hydrogen production rate, LSCF7328 membranes were sealed to the end of an  $\text{Al}_2\text{O}_3$  tube using an assembly described elsewhere [9]. During the measurements,  $\text{N}_2$  was bubbled through a water bath at a fixed temperature, and then was flowed over the hydrogen-generation side. The water's temperature was adjusted to control  $\text{pH}_2\text{O}$  on the steam side. A gas of 80%  $\text{H}_2$ /balance He was flowed over the oxygen-permeate side. A gas chromatograph (Hewlett-Packard 6890) was used to measure hydrogen concentrations in the gas stream at temperatures of  $600\text{--}900^\circ\text{C}$ .

Figure 9 plots the hydrogen production rate of three LSCF7328 thin films versus  $\text{pH}_2\text{O}$  on the hydrogen-generation side. The substrates for two films were made with carbon powder (20 wt.%) to increase their porosity, whereas the third film was prepared on a substrate made without carbon powder. Before they were coated with films, all substrates were fired in air for

10 h at 1050°C. After firing, the substrate made without carbon powder was semi-porous with a relative density of 82.4%, whereas substrates made with carbon powder had a relative density of 51.2%. Of the films on substrates made with carbon, one was coated with a porous Pt layer, and one was not. The thickness of each film, as measured by SEM, is given in the legend of Fig. 9.

The porosity of LSCF7328 substrates strongly affects the hydrogen production rate of LSCF7328 thin films (Fig. 9). For the two films not coated with porous Pt, the hydrogen production rate for  $p_{H_2O} = 0.5$  atm was  $3.0 \text{ cm}^3/\text{min}\cdot\text{cm}^2$  for the film on the relatively dense (82.4%) substrate made without any carbon, but was more than tripled ( $9.8 \text{ cm}^3/\text{min}\cdot\text{cm}^2$ ) for the film on the much more porous (51.2% dense) substrate made with carbon. The hydrogen production rate was even higher ( $11.4 \text{ cm}^3/\text{min}\cdot\text{cm}^2$ ) for the film on a porous substrate that was coated with porous Pt, even though the film was considerably thicker ( $50 \mu\text{m}$  vs.  $\approx 25 \mu\text{m}$  for the films not coated with porous Pt). Similarly, the hydrogen production rate of dense LSCF7328 disks increased when they were coated with porous Pt. This finding suggests that higher hydrogen production rates can be obtained by coating thinner ( $<25 \mu\text{m}$ ) LSCF7328 membranes with porous Pt.

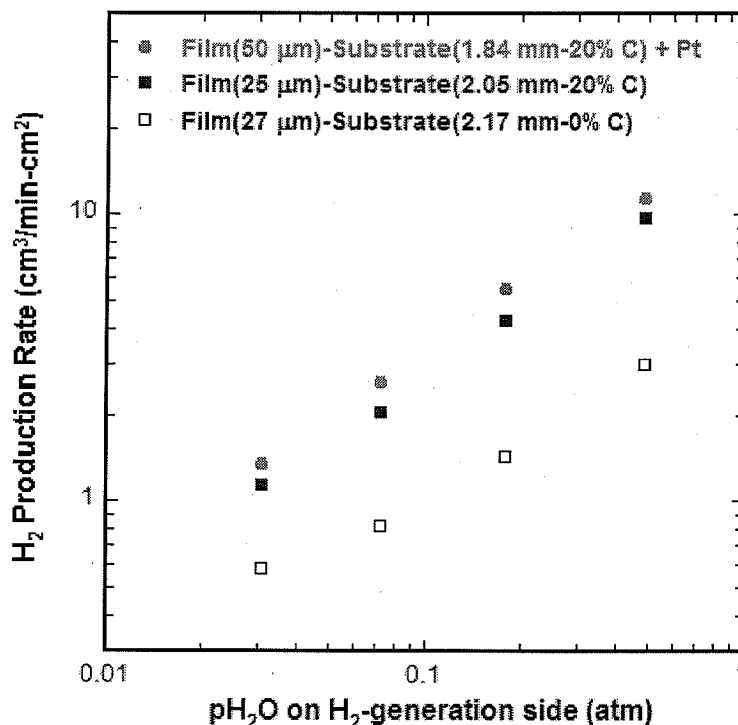
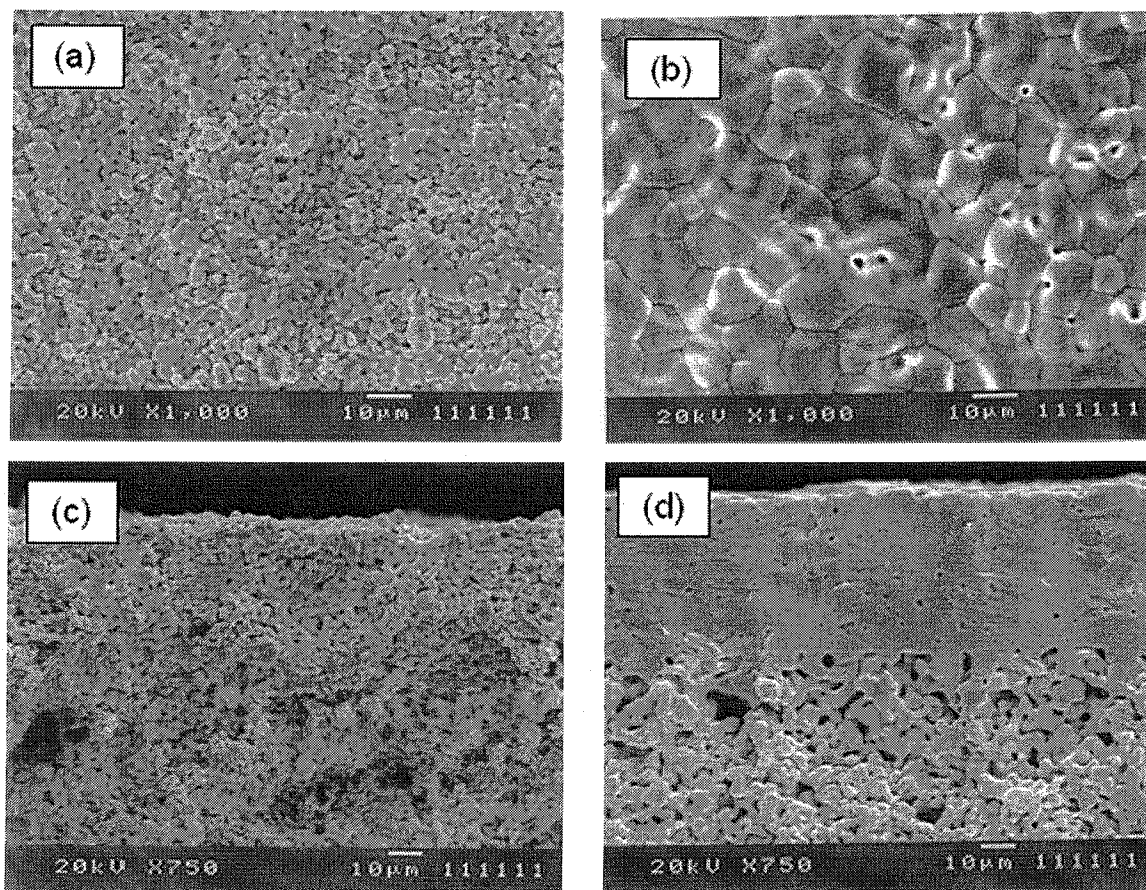


Fig. 9 Hydrogen production rate vs.  $p_{H_2O}$  at 900°C for LSCF7328 thin films on porous LSCF7328 substrates made with 20% carbon and dense LSCF7328 substrate made without carbon. Legend gives film and substrate thicknesses. Gas stream of 80%  $H_2$ /balance He was flowed on oxygen-permeate side.

We are also testing Sr-Fe-Ti-O<sub>x</sub> (SFT) membranes for low-temperature applications. Because it is known that Sr deficiency increases the stability of SFT in humidified atmospheres [10], we are investigating the effect of this deficiency on the hydrogen production rate under water splitting conditions. Figure 10 shows SEM micrographs of SrFe<sub>0.9</sub>Ti<sub>0.1</sub>O<sub>x</sub> (SFT1) and Sr<sub>0.95</sub>Fe<sub>0.9</sub>Ti<sub>0.1</sub>O<sub>x</sub> (SdFT1) films that were sintered in 100 ppm H<sub>2</sub>/balance N<sub>2</sub> for 5 h at 1300°C. Both films were made on porous SFT1 substrates that were prepared by using SFT1 powder mixed with 20 wt.% carbon. The powder mixture was uniaxially pressed (200 MPa) into disks that were pre-sintered in air for 5 h at 950°C to remove the carbon and provide the disks with mechanical integrity. Green films of SFT1 were made by casting an SFT1 colloid onto the porous substrate, while SdFT1 films were made by dip coating the substrate in a suspension of SdFT1 powder. Green films were then sintered in ≈100 ppm H<sub>2</sub>/balance N<sub>2</sub> for 5 h at 1300°C. Even though the films were sintered under the same conditions, the SdFT1 film appears denser than the SFT1 film in both the plan view of the surfaces (Figs. 10a/10b) and the cross-sectional view of fracture surfaces (Figs. 10c/10d).



*Fig. 10 SEM micrographs of SFT1 and SdFT1 disk-type thin films. Plan view of as-sintered (a) SFT1 and (b) SdFT1 films, and cross-sectional views of fracture surfaces from (c) SFT1 and (d) SdFT1 films.*

## Milestone 2. Fabricate and test tubular membranes for hydrogen production.

To be practical, OTMs must be available in a shape that has a large active area, such as tubes; therefore, we are developing methods for fabricating tubular membranes. In our initial effort, we fabricated dense, self-supporting SFC2 tubes with relatively thick ( $\approx 0.7$  mm) walls. Tubes were made by pressing SFC2 powder (Praxair Specialty Ceramics) in a cold isostatic press (Engineered Pressure Systems) in a rubber mold (Trexler Rubber) with a stainless steel mandrel at 10,000-15,000 psig. After pressing, the tube was sintered at 1150°C for 10 h in an argon atmosphere. Tubes produced by this method are typically 8-10 cm in length with an outside diameter of  $\approx 1$  cm and a membrane thickness of  $\approx 0.7$  mm. This method can be used to fabricate tubes that are open on both ends and tubes that are closed on one end.

Tubes are tested for pinholes and/or microcracks by checking for penetration of the film by IPA. In this test, the tube is filled with IPA, and the tube is examined for evidence that IPA is penetrating the film on its outer surface. Penetration of the film by even a small amount of IPA is visible as a darkening of the film and indicates that the tube contains cracks or interconnected porosity.

If an IPA-penetration test reveals no leakage, the tube's hydrogen production rate can be measured by a spring-loaded test fixture like that shown in Fig. 11. With this fixture, graphite gaskets are placed on the open ends of the tube, and the tube and gaskets are squeezed between an alumina tube and an alumina plate. If a tube passes the IPA test, it is sealed to a spring-loaded fixture and can be checked for leakage at room temperature by pressurizing the tube with 5 psi He and submerging it in IPA. If bubbling is not observed through the wall of the painted tube and is minimal at the gold ring used to seal the tube to the test fixture, the tube is placed into the reactor to measure its hydrogen production rate.

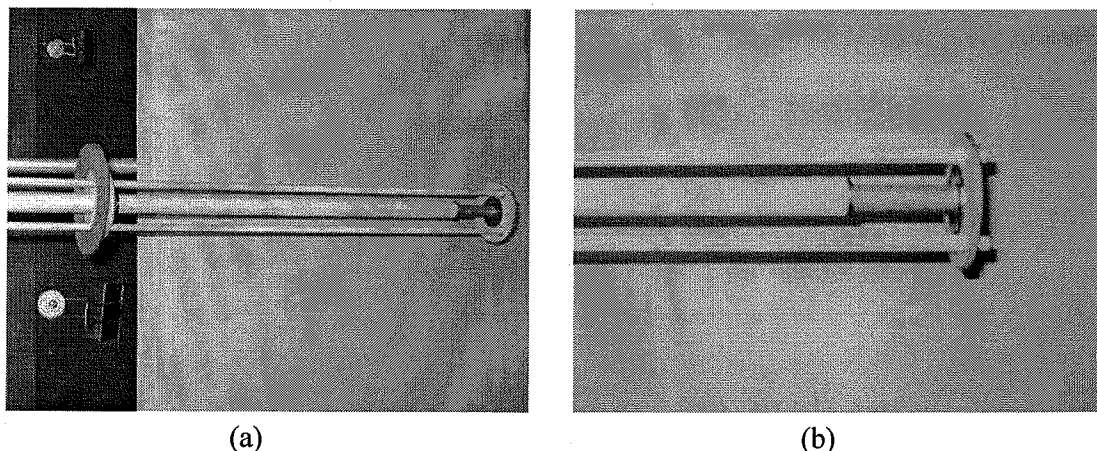


Fig. 11 Spring-loaded fixture (with tube in place) for measuring hydrogen production rate.

To test tubular membranes, UHP nitrogen was bubbled through water at a fixed temperature to control the  $p_{H_2O}$  and then was flowed over the hydrogen-generation side. The temperature of the water bath was adjusted to control  $p_{H_2O}$ . On the oxygen-permeate side of

the membrane, various gases (e.g., CO, 25% CO/75% CO<sub>2</sub>, or hydrogen-helium mixtures) were passed to drive oxygen diffusion through the OTM due to their reactivity with oxygen. The hydrogen-helium mixtures (4-80% H<sub>2</sub>) were prepared by mixing UHP hydrogen and UHP helium with mass flow controllers. The hydrogen production rate was measured with gas flow rates of 150-400 cm<sup>3</sup>/min at temperatures of 500-900°C. A Hewlett-Packard 6890 gas chromatograph was used to measure hydrogen concentrations on the hydrogen-generation side.

An SFC2 tube (length, ≈8 cm; outside diameter, ≈1 cm; membrane thickness, ≈0.7 mm; and surface area, ≈23.4 cm<sup>2</sup>) was prepared for testing. The tube's hydrogen production rate (Fig. 12) was measured at 900°C versus p<sub>H<sub>2</sub>O</sub> (0.03-0.49 atm) on the hydrogen-generation side with 80% H<sub>2</sub>/balance He flowing on the oxygen-permeate side. Measurements were made for two sets of gas flow rates: (1) 150 cm<sup>3</sup>/min on both sides of the membrane and (2) 400 cm<sup>3</sup>/min on the hydrogen-generation side and 200 cm<sup>3</sup>/min on the oxygen-permeate side.

The hydrogen production rate for the tube was lower than that of a disk-type SFC2 membrane with comparable thickness under identical experimental conditions using gas flow rates of 150 cm<sup>3</sup>/min on both sides of the membrane. With p<sub>H<sub>2</sub>O</sub> = 0.49 atm, the tube had a hydrogen production rate of ≈1.5 cm<sup>3</sup>/min-cm<sup>2</sup>, whereas a 0.62-mm-thick SFC2 disk [11] had a hydrogen production rate >5 cm<sup>3</sup>/min-cm<sup>2</sup>. The main reason for the tube's low hydrogen production rate is believed to be concentration polarization caused by the accumulation of hydrogen on the hydrogen-generation side. This hypothesis was confirmed by the increase in hydrogen production rate that occurred when the flow rates were increased to 400 cm<sup>3</sup>/min on the hydrogen-generation side and 200 cm<sup>3</sup>/min on the oxygen-permeate side.

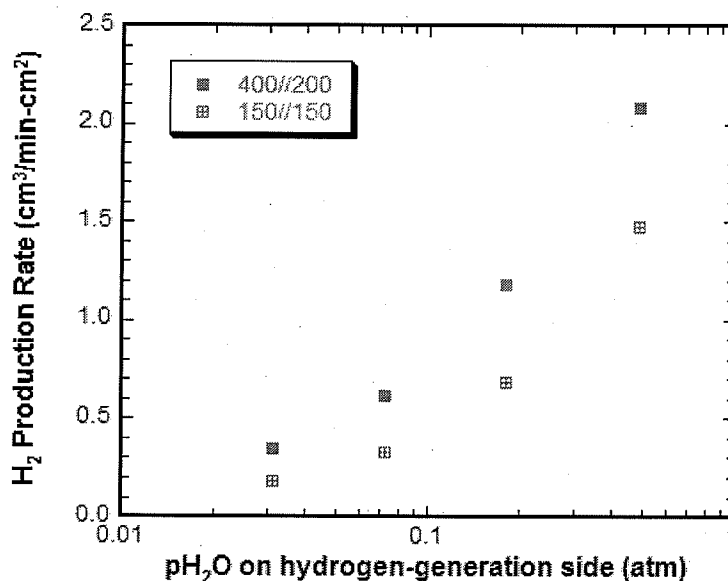


Fig. 12 Hydrogen production rate at 900°C vs. p<sub>H<sub>2</sub>O</sub> on hydrogen-generation side of SFC2 tube with 80% H<sub>2</sub>/He on oxygen-permeate side. Inset gives gas flow rates, e.g., 400//200 means 400 cm<sup>3</sup>/min of N<sub>2</sub>/H<sub>2</sub>O on hydrogen-generation side and 200 cm<sup>3</sup>/min of 80% H<sub>2</sub>/He on oxygen-permeate side.

The hydrogen production rate was measured for the SFC2 tube in the temperature range 500-900°C with  $p_{H_2O} = 0.03$  atm on the hydrogen-generation side and 80%  $H_2$ /balance He on the oxygen-permeate side. The results are plotted versus inverse temperature in Fig. 13. As seen previously with SFC2 disks [12], the hydrogen production rate drops sharply for temperatures below  $\approx 825^\circ\text{C}$  as SFC2 undergoes a phase transition. Due to the low hydrogen production rate caused by the phase transition, OTMs made of SFC2 are considered unsuitable for applications at  $< 825^\circ\text{C}$ . At temperatures  $> 850^\circ\text{C}$ , however, SFC2 shows the highest hydrogen production rate measured to date and is a good candidate for OTM applications.

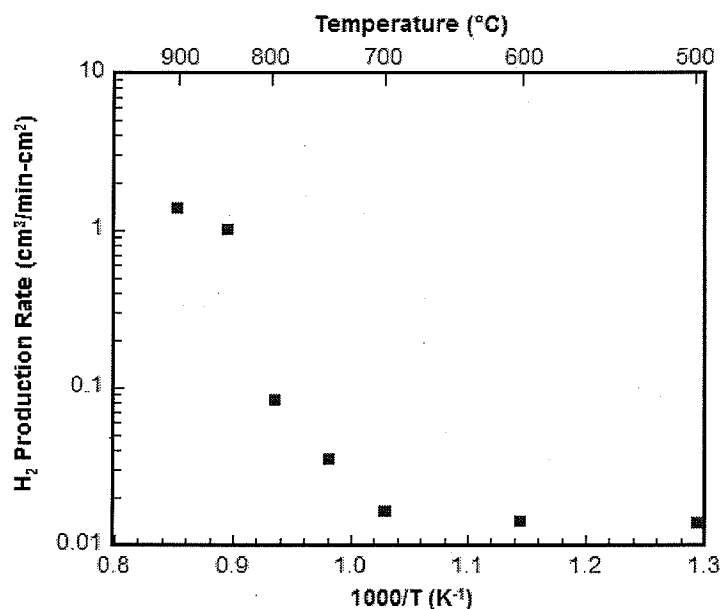


Fig. 13 Hydrogen production rate of SFC2 tube vs. inverse temperature using 80%  $H_2$ /balance He on oxygen-permeate side and humidified  $N_2$  ( $p_{H_2O} = 0.49$  atm) on hydrogen-generation side.

Figure 14 shows the hydrogen production rate versus  $p_{H_2O}$  on the hydrogen-generation side of the SFC2 tube for three gases on the oxygen-permeate side: 80%  $H_2$ /balance He, CO, and 25% CO/75%  $CO_2$ . The flow rate of each gas was 200 ml/min on the oxygen-permeate side. Gas on the hydrogen-generation side consisted of UHP nitrogen bubbled through water at a rate of 400 ml/min. The  $p_{H_2O}$  on the hydrogen-generation side was fixed by controlling the temperature of the water bath. As expected, for all three gases on the oxygen-permeate side, the hydrogen production rate increased as  $p_{H_2O}$  increased on the hydrogen-generation side. The hydrogen production rate decreased as the gas on the oxygen-permeate side was changed from 80%  $H_2$ /balance He to CO, and then to 25% CO/75%  $CO_2$ , because the change in gas decreased the driving force for oxygen diffusion through the membrane. The driving force for oxygen diffusion decreased with the change in gas, because the reactivity of the gas toward oxygen decreased, thereby increasing the oxygen chemical potential on the oxygen-permeate side.

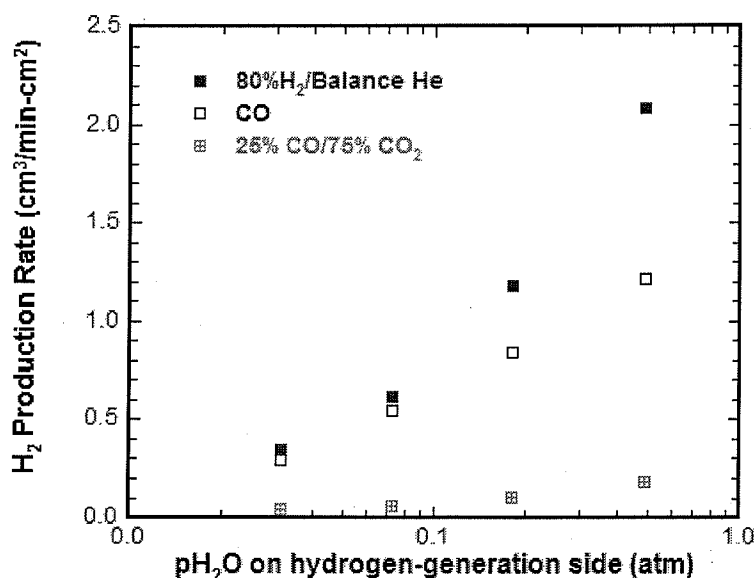
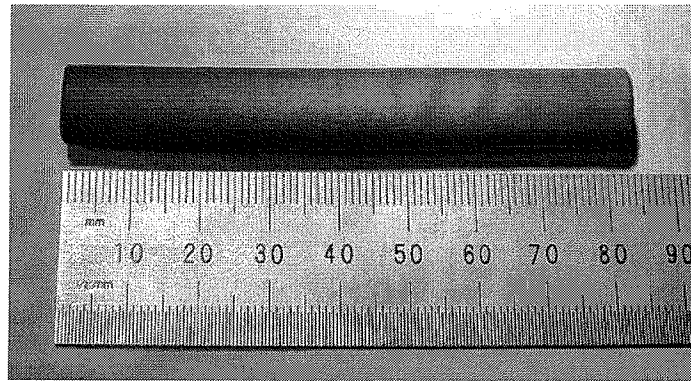


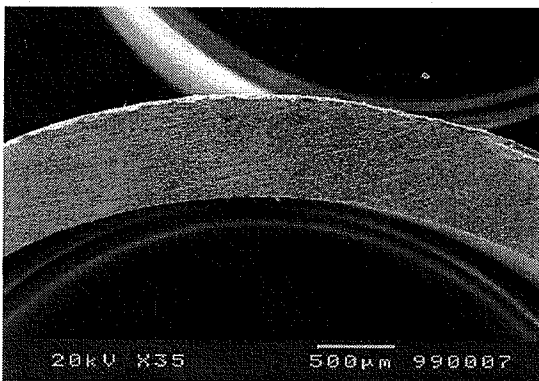
Fig. 14 Hydrogen production rates vs.  $p_{H_2O}$  on hydrogen-generation side of SFC2 tube at 900 °C using 80%  $H_2/He$ , CO, and 25% CO/75%  $CO_2$  on oxygen-permeate side.

Another approach for fabricating tubular OTMs is the paste-painting technique that we use to fabricate thin films of hydrogen transport membranes. In this approach, we first produce porous support tubes in a cold isostatic press (Engineered Pressure Systems) by pressing SFC2 powder mixed with 20 wt.% carbon in a rubber mold (Trexler Rubber) with a stainless steel mandrel at 10,000-15,000 psig. After pressing, the support tube is pre-sintered at 950°C for 5 h in ambient air to remove the carbon and provide the tube with sufficient mechanical strength for subsequent handling. The pre-sintered tube is then painted on the outside surface with a paste containing SFC2 powder, and it is sintered for 10 h at 1200°C in 100 ppm  $H_2/N_2$ , giving a dense SFC2 film on a tubular porous support. Tubes produced by this method are typically 8-10 cm in length with an outside diameter of  $\approx 1$  cm and a membrane thickness of 25-50  $\mu m$ . Figure 15 shows an SFC2 tube made by this method.

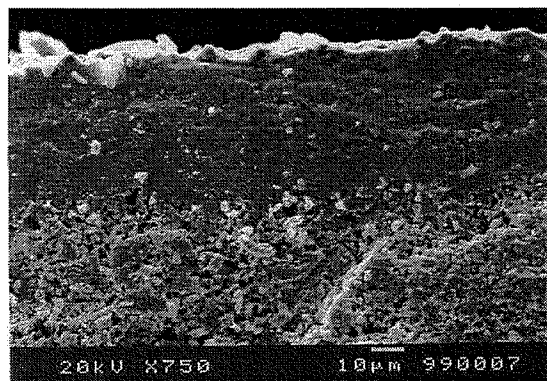
The hydrogen production rate of a tubular SFC2 thin film (film thickness,  $\approx 40 \mu m$ ) was measured over the range 700-900°C (Fig. 16). During the measurements, 80%  $H_2$ /balance He was flowed on the oxygen-permeate side of the tube while humidified ( $p_{H_2O} = 0.49$  atm) UHP nitrogen was flowed on the steam side. Relatively high gas flow rates (500  $cm^3/min$ ) were used on both sides of the tube to minimize concentration polarization. As a reference, the hydrogen production rates are also shown for a relatively thick ( $\approx 0.7$  mm), self-supported SFC2 tube that was tested with gas flow rates of 150  $cm^3/min$  on both sides. Both tubes show a sharp drop in hydrogen production rate at  $\approx 825^\circ C$  due to the phase transition for SFC2.



(a)



(b)



(c)

Fig. 15 Thin-film SFC2 tube made by paste-painting technique: a) photograph, b) "low" magnification cross-sectional view, and c) "high" magnification cross-sectional view.

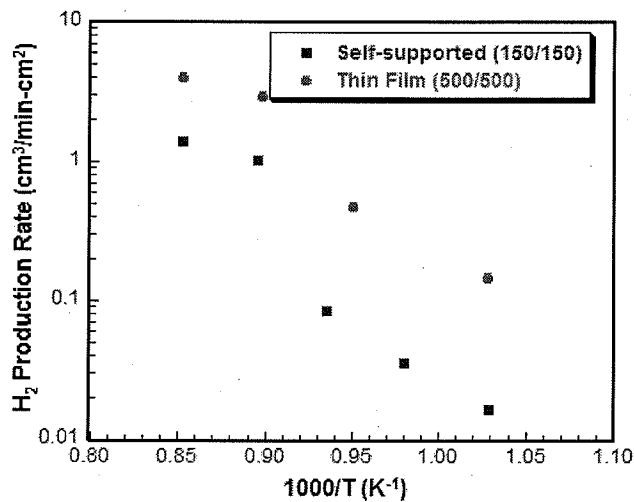


Fig. 16 Hydrogen production rate vs. temperature for thin-film and self-supported SFC2 tubes, measured with N<sub>2</sub> (pH<sub>2</sub>O = 0.49 atm) on steam side and 80% H<sub>2</sub>/balance He on oxygen-permeate side. Legend gives flow rates on steam and oxygen-permeate sides of tube.

Figure 17 shows the hydrogen production rate at 900°C versus  $p_{H_2O}$  on the steam side of a tubular SFC2 thin film (thickness,  $\approx 40 \mu\text{m}$ ; surface area,  $\approx 21.3 \text{ cm}^2$ ) and a self-supporting SFC2 tube with 80%  $H_2$ /balance He flowing on the oxygen-permeate side. As expected, the  $H_2$  production rate increased with increasing  $p_{H_2O}$  for both types of tube, but the thin-film tube had a higher hydrogen production rate for all values of  $p_{H_2O}$ . With  $p_{H_2O} = 0.49 \text{ atm}$ , the thin film gave a hydrogen production rate of  $\approx 4.3 \text{ cm}^3/\text{min}\cdot\text{cm}^2$ , which was about three times higher than that of the self-supported tube ( $\approx 1.5 \text{ cm}^3/\text{min}\cdot\text{cm}^2$ ). The thin-film tube gave a higher production rate versus  $p_{H_2O}$  (Fig. 17) and temperature (Fig. 16) due to its smaller thickness and because it was tested with higher gas flow rates. The effects of membrane thickness and gas flow rate on these data cannot be separated.

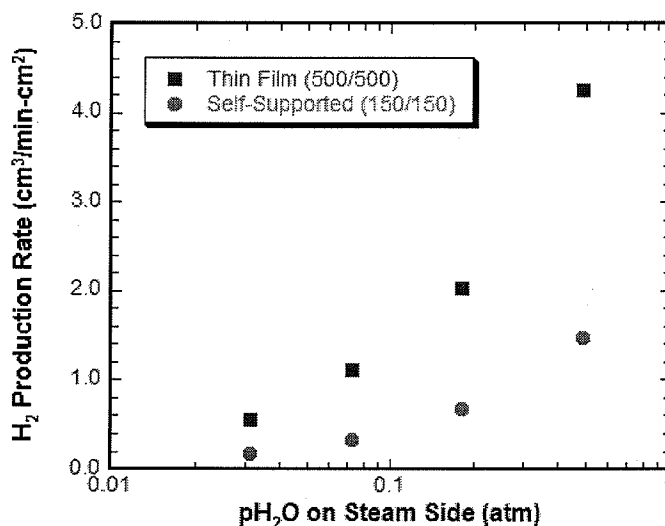


Fig. 17 Hydrogen production rate at 900 °C vs.  $p_{H_2O}$  on steam side of thin-film and self-supported SFC2 tubes, measured with 80%  $H_2$ /He on oxygen-permeate side. Legend gives flow rates on steam/oxygen-permeate sides of tube.

To investigate the effect of gas flow rates, we measured the hydrogen production rate of a thin-film SFC2 tube while varying the gas flow rate on both sides of the tube. Table 1 summarizes the effect of the gas flow rates on the area-specific hydrogen production rate ( $\text{cm}^3/\text{min}\cdot\text{cm}^2$ ), the “total” hydrogen production rate, i.e., for the entire tube ( $\text{cm}^3/\text{min}$ ), and the water conversion rate (the ratio of “hydrogen out” to “water in”). Figure 18 plots the effects of the gas flow rates on the total hydrogen production rate. 80%  $H_2$ /balance He was flowed on the oxygen-permeate side during all measurements, while humidified  $N_2$  was flowed on the steam side. With a fixed flow rate (150  $\text{cm}^3/\text{min}$ ) on the oxygen-permeate side, the tube hydrogen production rate increased linearly as the flow rate of  $N_2$  ( $p_{H_2O} = 0.03 \text{ atm}$ ) increased from 150 to 500  $\text{cm}^3/\text{min}$  on the steam side. However, with the flow rate on the steam side fixed at 500  $\text{cm}^3/\text{min}$ , the tube hydrogen production rate varied only slightly when the flow rate was increased from 150 to 500  $\text{cm}^3/\text{min}$  on the oxygen-permeate side. This indicates that the hydrogen production rate is limited more by flow rate on the steam side than the oxygen-permeate side.

Table 1. Effect of gas flow rates on hydrogen production rate of tubular SFC2 thin film (film thickness  $\approx 40 \mu\text{m}$ ).

80% H <sub>2</sub> /He - Wet N <sub>2</sub> (pH <sub>2</sub> O = 0.03 atm)				
Gas flow rate (cm <sup>3</sup> /min)	150 - 150	150 - 300	150 - 500	500 - 500
Tube HPR <sup>a</sup> (cm <sup>3</sup> /min)	5.1	7.9	11.0	11.9
Conversion rate (%) <sup>b</sup>	100.0	93.8	76.3	82.6
Area-specific HPR <sup>a</sup> (cm <sup>3</sup> /min-cm <sup>2</sup> )	0.24	0.37	0.52	0.56
80% H <sub>2</sub> /He // Wet N <sub>2</sub> (pH <sub>2</sub> O = 0.48 atm)				
Gas flow rate (cm <sup>3</sup> /min)	700 - 150	700 - 300	700 - 500	700 - 700
Tube HPR <sup>a</sup> (cm <sup>3</sup> /min)	50.5	61.1	81.8	84.2
Conversion rate (%) <sup>b</sup>	71.3	44.7	34.3	24.7
Area-specific HPR <sup>a</sup> (cm <sup>3</sup> /min-cm <sup>2</sup> )	2.37	2.87	3.84	3.95

<sup>a</sup> HPR = hydrogen production rate.

<sup>b</sup> Conversion rate = moles H<sub>2</sub> out/moles H<sub>2</sub>O in.

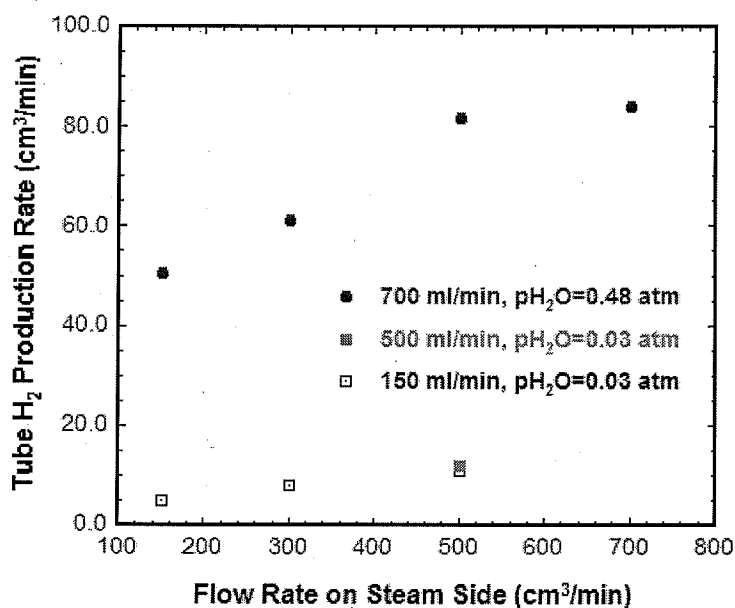


Fig. 18 Hydrogen production rate of thin-film SFC2 tube vs. flow rate of humidified N<sub>2</sub> on steam side of tube. Flow rate of 80% H<sub>2</sub>/balance He on oxygen-permeate side and pH<sub>2</sub>O on steam side are given in legend.

Similar results were obtained with higher  $p_{\text{H}_2\text{O}}$  (0.48 atm) on the steam side of the tube and higher flow rate ( $700 \text{ cm}^3/\text{min}$ ) of 80%  $\text{H}_2$ /balance He on the oxygen-permeate side. As the flow rate on the steam side was increased from 150 to  $500 \text{ cm}^3/\text{min}$ , the total hydrogen production rate increased roughly linearly. Further increasing the flow rate on the steam side to  $700 \text{ cm}^3/\text{min}$  increased the total hydrogen production rate only slightly. These results indicate that, for the tube tested here, concentration polarization effects were largely eliminated with a flow rate  $>500 \text{ cm}^3/\text{min}$  on the steam side.

### **Milestone 3. Test concept of using coal combustion to drive water dissociation for hydrogen production.**

To demonstrate the concept that combustion of coal can drive hydrogen production via water dissociation, we measured the hydrogen production rate of LSCF7328 thin films in tests using  $\text{CO}/\text{CO}_2$  gas mixtures on the oxygen-permeate side. The methods for making LSCF7328 powder, substrates, and thin films are described in the section regarding Milestone 1. The hydrogen production rates were determined with the LSCF7328 films sealed to the end of an  $\text{Al}_2\text{O}_3$  tube by using an assembly described elsewhere [9].

During the hydrogen production rate measurements, humidified nitrogen was flowed over the hydrogen-generation side, while 80%  $\text{H}_2$ /balance He or a  $\text{CO}/\text{CO}_2$  mixture was flowed over the oxygen-permeate side. To fix the  $p_{\text{H}_2\text{O}}$  on the hydrogen-generation side, the nitrogen was bubbled through a water bath at a fixed temperature before it was flowed over the membrane. Hydrogen on the oxygen-permeate side reacts with oxygen as it diffuses through the film, thus creating a low  $p_{\text{O}_2}$  on the oxygen-permeate side and establishing a  $p_{\text{O}_2}$  gradient across the membrane. The hydrogen/helium mixture was used on the oxygen-permeate side only as a model gas to evaluate the effects of membrane thickness, surface coating, and conditions of the porous support structure. To simulate the process of using coal combustion to drive hydrogen production via water dissociation,  $\text{CO}/\text{CO}_2$  gas mixtures were flowed on the oxygen-permeate side. A gas chromatograph (Hewlett-Packard 6890) was used to measure hydrogen concentrations in the gas stream at temperatures of  $600\text{-}900^\circ\text{C}$ .

To demonstrate that combustion of coal can drive hydrogen production via water dissociation, we measured the hydrogen production rate of a supported LSCF7328 thin film (film thickness  $\approx 22 \mu\text{m}$ ) while a simulated coal combustion atmosphere was flowed on the oxygen-permeate side. The hydrogen production rate was measured at  $600\text{-}900^\circ\text{C}$  while flowing humidified  $\text{N}_2$  ( $p_{\text{H}_2\text{O}} = 0.49 \text{ atm}$ ) on the hydrogen-generation side and  $\text{CO}/\text{CO}_2$  gas mixtures on the oxygen-permeate side. First, to compare the performance of the film to other LSCF7328 films, the hydrogen production rate was measured using 80%  $\text{H}_2$ /balance He on the oxygen-permeate side. The hydrogen production rate at  $900^\circ\text{C}$  ( $9.0 \text{ cm}^3/\text{min}\text{-cm}^2$ ) was close to the value ( $9.8 \text{ cm}^3/\text{min}\text{-cm}^2$ ) reported above (Fig. 9) for another LSCF7328 film with similar thickness and tested under identical conditions, indicating that the properties of the LSCF7328 films are reproducible.

The  $H_2$  production rate for the LSCF7328 thin film is plotted (Fig. 19) versus the CO concentration in the simulated coal combustion atmosphere on the oxygen-permeate side. The CO concentration was balanced with either  $CO_2$  or He for the measurements at 600 and 900°C, but was balanced with only  $CO_2$  for the measurements at 700 and 800°C. Dissociation of  $CO_2$  increases the  $pO_2$  in  $CO/CO_2$  mixtures, relative to  $CO/He$  mixtures with the same nominal CO concentration; consequently, the driving force for oxygen diffusion through the membrane is smaller with a  $CO/CO_2$  mixture on the oxygen-permeate side. As a result, a  $CO/CO_2$  mixture on the oxygen-permeate side gives a smaller hydrogen production rate than does a  $CO/He$  mixture with the same nominal CO concentration.

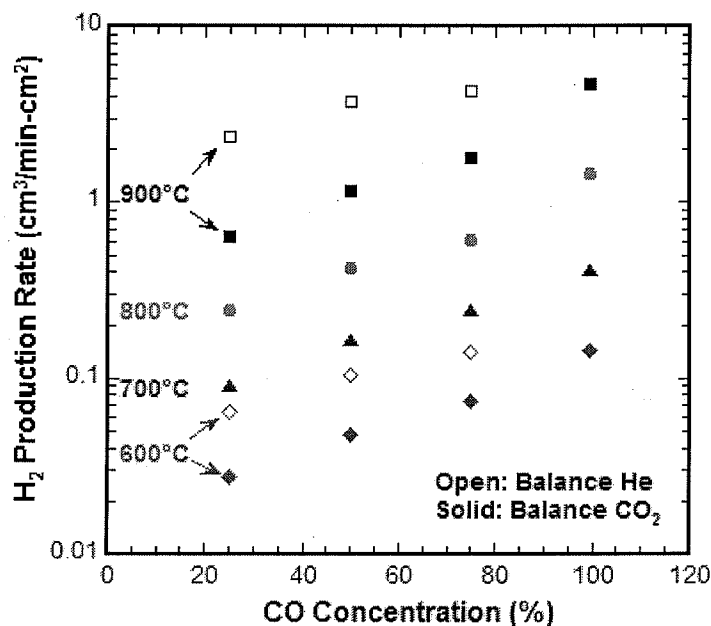


Fig. 19 Hydrogen production rate of LSCF7328 thin film on porous LSCF7328 substrate with 20% C vs. temperature and CO concentration in gas on oxygen-permeate side with balance of He (open symbols) or  $CO_2$  (solid symbols).  $N_2$  ( $p_{H_2O} = 0.49$  atm) flowed on hydrogen-generation side.

Figure 20 shows the hydrogen production rate of the LSCF7328 thin-film membrane versus the CO concentration on its oxygen-permeate side. With CO (99.5% purity) on the oxygen-permeate side, a hydrogen production rate of  $\approx 4.7$   $cm^3/min-cm^2$  was measured at 900°C, showing that hydrogen can be produced at a significant rate when gases from coal combustion are used to drive the dissociation of water. As the CO concentration decreased on the oxygen-permeate side, the  $pO_2$  increased, causing a decrease in the driving force for oxygen diffusion from the hydrogen-generation side. As a result, the hydrogen production rate decreased as the CO concentration decreased. Because oxygen diffusion is thermally activated, the hydrogen production rate also decreased as temperature decreased. The CO concentration had a similar effect on the hydrogen production rate of an SFC2 tubular membrane (Fig. 14).

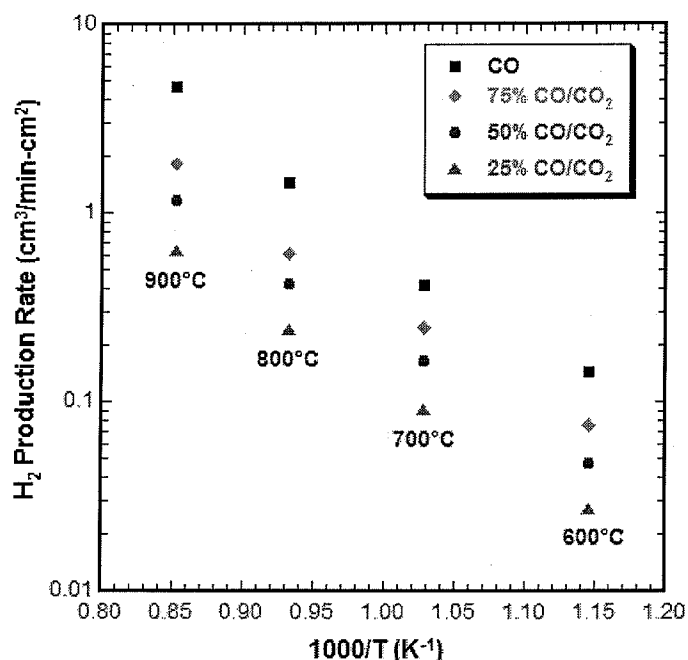


Fig. 20 Hydrogen production rate of LSCF7328 thin film on porous LSCF7328 substrate made with 20% C vs. inverse temperature using various CO/CO<sub>2</sub> gas mixtures on oxygen-permeate side. N<sub>2</sub> (pH<sub>2</sub>O = 0.49 atm) flowed on hydrogen-generation side.

#### Milestone 4. Evaluate chemical stability of the membranes.

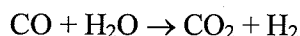
In addition to the critical need for producing hydrogen at a high rate, OTMs must be chemically stable for extended periods under the reaction conditions for producing hydrogen, i.e., high pressures of steam on the hydrogen-generation side and a corrosive reducing gas on the oxygen-permeate side. To test the chemical stability of an SFC2 tube, we measured its hydrogen production rate for >700 h while flowing a variety of reducing gases on the oxygen-permeate side. The reducing gases included CO/CO<sub>2</sub> mixtures that were mixed in the laboratory and CO/CO<sub>2</sub>-containing mixtures that were produced by flowing ethanol vapor on the oxygen-permeate side.

A self-supporting tube was made for the chemical stability study by pressing SFC2 powder (Praxair Specialty Ceramics) at 10,000-15,000 psig in a rubber mold (Trexler Rubber) with a stainless steel mandrel in a cold isostatic press (Engineered Pressure Systems). After being pressed, the tube was sintered at 1150°C for 10 h in an argon atmosphere. After firing, the tube had a length of ≈6 cm with an outside diameter of ≈1 cm and a membrane thickness of ≈0.7 mm. The tube was tested for pinholes and/or microcracks by filling it with IPA and inspecting for penetration by the IPA. When even a small amount of IPA penetrates the tube, it is easily visible as darkening of the tube and indicates the presence of cracks and/or interconnected porosity. After passing the IPA test, the tube was mounted for hydrogen production rate measurements on a spring-loaded test fixture like that shown in Fig. 11.

To measure the tube's hydrogen production rate, humidified UHP nitrogen was flowed on the hydrogen-generation ("steam") side of the tube. The  $p_{H_2O}$  was controlled by passing the nitrogen through water at a fixed temperature. On the oxygen-permeate side, we passed either a CO/CO<sub>2</sub> mixture prepared with mass flow controllers or an inert gas (He or N<sub>2</sub>) saturated with ethanol (EtOH) at room temperature to give an ethanol partial pressure ( $p_{EtOH}$ ) of 0.05 atm. The actual composition of "ethanol" in the experiments was 95% ethanol and 5% water (by volume). Gas flow rates were controlled in the range 150-400 cm<sup>3</sup>/min. A Hewlett-Packard 6890 gas chromatograph was used to analyze the gas composition formed by the ethanol vapors on the oxygen-permeate side of the tube and the hydrogen concentrations that were produced via water dissociation on the steam side.

The hydrogen production rate was measured for ≈100 h at 900°C in tests using an SFC2 tube (surface area ≈23.4 cm<sup>2</sup>) with N<sub>2</sub> (0.03 atm H<sub>2</sub>O) on the steam side and He (0.05 atm EtOH) on the oxygen-permeate side, both gases flowing at a rate of 150 cm<sup>3</sup>/min. The hydrogen production rate was then measured for ≈600 h while flowing N<sub>2</sub> (0.03 atm H<sub>2</sub>O) on the steam side at 400 cm<sup>3</sup>/min and He (0.05 atm EtOH), 25% CO/balance CO<sub>2</sub>, or 100% CO on the oxygen-permeate side at 200 cm<sup>3</sup>/min. After testing the tube's performance with various gases on the oxygen-permeate side, its hydrogen production rate was measured again under the initial conditions, i.e., with N<sub>2</sub> (0.03 atm H<sub>2</sub>O) and He (0.05 atm ethanol) both flowing at a rate of 150 cm<sup>3</sup>/min.

Table 2 shows the measured and calculated concentrations of products that were formed from ethanol vapor on the oxygen-permeate side of the membrane. No ethanol was detected at the reactor outlet, in agreement with the calculations, which predict >99.9% conversion of ethanol. Whereas the calculations predict negligible formation of CO<sub>2</sub>, significant amounts of CO<sub>2</sub> were measured. The higher-than-predicted concentration of CO<sub>2</sub> may result from reaction between CO and oxygen that permeates the tube after it is formed by water splitting on the other side of the tube. The measured hydrogen concentration was also higher than the hydrogen concentration predicted by calculation. The high CO<sub>2</sub> and H<sub>2</sub> concentrations (compared to calculated values) may also be attributable to the water-gas shift reaction:



The measured concentrations of ethylene and ethane were also higher than the calculated values, and the carbon balance was <1. After the test was complete, coke was found inside of the alumina tubes in both reactors, explaining why the carbon balance was <1.

Table 2. Composition of atmosphere on oxygen-permeate side of SFC2 tube during test of tube's chemical stability at 900°C.

	H <sub>2</sub>	CO	CH <sub>4</sub>	CO <sub>2</sub>	C <sub>2</sub> H <sub>4</sub>	C <sub>2</sub> H <sub>6</sub>	Carbon Balance <sup>a</sup>
Calculated	5.87	5.03	4.19	1*10 <sup>-5</sup>	0.15	0.002	---
Disk	6.50	3.92	2.27	0.44	0.85	0.02	0.87
Tube	7.26	3.81	1.18	0.93	0.90	0.02	0.86

<sup>a</sup> The measured total moles of carbon (carbon-containing gases) divided by the moles of carbon put into the reactor as ethanol.

The hydrogen production rate of the SFC2 tube (Fig. 21) was first measured for  $\approx 100$  h with He (0.05 atm EtOH) on the oxygen-permeate side and  $N_2$  (0.03 atm  $H_2O$ ) on the steam side, both gases flowing at a rate of  $150 \text{ cm}^3/\text{min}$ . Considering that the uncertainty in hydrogen production rate measurements is  $\approx \pm 5\%$ , the results appeared stable. Using higher gas flow rates, we then measured the tube's hydrogen production rate while flowing a highly reducing gas (100% CO), followed by ethanol-containing He and then a mixture that contained a high concentration of  $CO_2$ . The higher gas flow rates increased the hydrogen production rate significantly, probably by reducing concentration polarization along the tube. After measuring the hydrogen production rate under these conditions, we measured it again under the "initial" conditions, i.e. with He (0.05 atm EtOH) on the oxygen-permeate side and  $N_2$  (0.03 atm  $H_2O$ ) on the steam side flowing at a rate of  $150 \text{ cm}^3/\text{min}$ . As shown by the last two data, the hydrogen production rate after  $>700$  h of testing was unchanged from its value during the first  $\approx 100$  h of testing, indicating that SFC2 had remained stable.

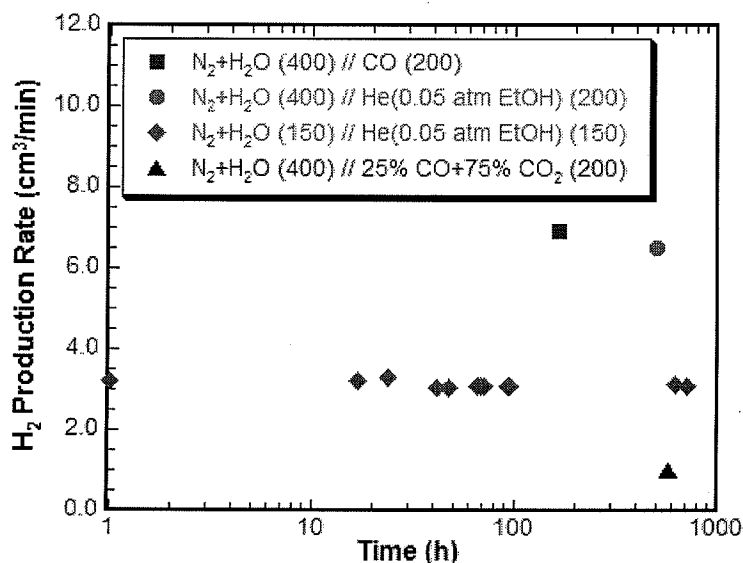


Fig. 21 Hydrogen production rate at  $900^\circ\text{C}$  for SFC2 during test of its chemical stability.  $N_2$  (0.03 atm  $H_2O$ ) flowed on hydrogen-generation side, and various gases on oxygen-permeate side. Gas flow rates ( $\text{cm}^3/\text{min}$ ) are given in parentheses.

## V. FUTURE WORK

We will continue efforts to develop new OTM materials with enhanced ability to produce hydrogen via coal/coal gas-assisted water splitting. In these efforts, we will investigate entirely new membrane compositions and apply methods described in this report to enhance the hydrogen production rate of the OTMs being developed. Based on the principles of solid-state chemistry, we will prepare and test novel materials thought to have potential for high hydrogen production rates. To increase the hydrogen production rates of existing OTM materials, we will continue to improve methods for reproducibly fabricating membranes with thickness  $< \approx 25 \mu\text{m}$ , and we will coat membranes with porous layers,

working to optimize microstructural features of the porous layers, such as porosity and pore size. When the hydrogen production rate is significantly influenced by sintering conditions, we will optimize the sintering process to enhance hydrogen production.

We will fabricate and test tubular thin-film OTMs in FY2009 to demonstrate that OTMs with a significant hydrogen production rate are practical for large-scale industrial applications. Tubes are practical for large-scale industrial processes due to their large active area and the relative ease of their fabrication and gas-manifolding. To enhance the hydrogen production rates of tubular thin films, we will develop methods to coat both of the tube's surfaces with porous layers.

Tubular thin films will be used to demonstrate the concept of using coal combustion to drive water dissociation for hydrogen production. In this concept, coal is combusted on one side of an OTM, while water splitting produces hydrogen on the other side. During FY 2008, we demonstrated the concept using disk-shaped LSCF7328 thin films with CO/CO<sub>2</sub> gas mixtures to simulate the atmosphere produced by coal combustion. This concept would reduce the number of steps needed to produce hydrogen from coal and, thereby, increase the process efficiency. The hydrogen produced would be physically separated from carbon dioxide and all other impurities; therefore, hydrogen purification would be simpler and more cost-effective. Gas separation costs would be reduced because the OTM contains no precious metals. Because coal combustion is exothermic, the process would supply heat that is required for water splitting. In addition, the waste stream from the proposed process is ideal for sequestration, because it is rich in carbon dioxide. During FY 2009, we will use CO/CO<sub>2</sub> gas mixtures to test the possibility of employing this concept at low temperatures ( $\leq 700^{\circ}\text{C}$ ).

Good chemical stability is a critical requirement for OTMs due to the high temperatures and corrosive environments they will encounter; therefore, we will continue evaluating the chemical stability of OTMs in FY 2009. We will test the chemical and mechanical stability of OTMs in longer (up to  $\approx 1000$  h) exposures to industrially useful conditions, e.g., the atmospheres and temperatures that are typical for coal combustion and coal gasification. We will study the effect of syngas components on the hydrogen production rate of OTMs in the presence of H<sub>2</sub>S and without H<sub>2</sub>S. To assess the extent and course of reaction between the membrane and the atmosphere, the microstructure of membranes will be examined before and after exposures to industrial conditions.

We will evaluate process issues and economics as technical progress warrants. As directed by NETL's program managers, we will make contacts and hold discussions with potential collaborators. We will work with NETL's in-house R&D team and their Systems Engineering group to validate the process concept and assess the techno-economics of using OTMs to produce hydrogen by water splitting. We will provide technical input and engineering data to the NETL team to develop models for process viability and for thermal management studies.

## **PUBLICATIONS, PATENTS, AND PRESENTATIONS**

- Hydrogen Production by High-Temperature Water Splitting Using Mixed Oxygen Ion-Electron Conducting Membranes, Proc. 201<sup>st</sup> Electrochem. Soc. Mtg., Philadelphia, PA, May 12-17, 2002.
- Method for Generating Hydrogen by Catalytic Decomposition of Water, U.S. Patent 6,468,499, Oct. 22, 2002.
- Hydrogen Production by Water Splitting Using Mixed Conducting Membranes, Proc. National Hydrogen Assoc. 14<sup>th</sup> Annual U.S. Hydrogen Meeting, Washington, DC, March 4-6, 2003.
- Hydrogen Production by Water Dissociation Using Mixed-Conducting Membranes, presented at 225<sup>th</sup> Amer. Chem. Soc. Natl. Mtg., Fuel Chemistry Div., New Orleans, March 23-27, 2003.
- Hydrogen Production by Water Dissociation Using Oxygen-Permeable Cermet Membranes, presented at 105<sup>th</sup> Ann. Mtg. of Amer. Ceram. Soc., Nashville, April 27-30, 2003.
- Hydrogen Production by Water Dissociation Using Mixed Conducting Membranes, presented at Second Information Exchange Meeting on Nuclear Production of Hydrogen, Argonne Natl. Lab., Oct. 2-3, 2003.
- Use of Mixed Conducting Membranes to Produce Hydrogen by Water Dissociation, Intl. J. of Hydrogen Energy, 29, 291-296 (2004).
- Hydrogen Production from Water Splitting Using Mixed Oxygen Ion-Electron Conducting Membranes, U.S. Patent 6,726,893, Apr. 27, 2004.
- Hydrogen Production by Water Dissociation Using Mixed-Conducting Ceramic Membranes, Proc. of National Hydrogen Association's 15<sup>th</sup> Annual U.S. Hydrogen Energy Conf., Los Angeles, CA, April 27-30, 2004.
- Hydrogen Production from Water Using Mixed-Conducting Ceramic Membranes, presented at 15<sup>th</sup> World Hydrogen Energy Conf., Yokohama, Japan, June 27-July 2, 2004.
- Development of Dense Ceramic Membranes for Hydrogen Production and Separation, presented at American Soc. for Materials--Annual Materials Solution Conf., Columbus, OH, Oct. 18-21, 2004.
- Hydrogen Production by Water Splitting Using Dense Thin-Film Cermet Membranes, presented at Fall Meeting of Materials Research Society, Boston, Nov. 28-Dec. 2, 2005.
- Hydrogen Production by Water Dissociation Using Mixed Oxygen Ion-Electron Conducting Membranes, presented at Electrochem. Soc. 2005 Fall Mtg., Los Angeles, Oct. 16-21, 2005.
- Hydrogen Production by Water Dissociation Using Mixed-Conducting Dense Ceramic Membranes, invited presentation at Amer. Chem. Soc. 231<sup>st</sup> Natl. Mtg., Atlanta, March 26-30, 2006.
- Hydrogen Production by High-Temperature Water Splitting Using Electron-Conducting Membranes, U.S. Patent 7,087,211, Aug. 8, 2006.
- Mixed-Conducting Membranes for Hydrogen Production and Separation, presented at 2006 MRS Fall Meeting, Boston, MA, Nov. 27 - Dec 1, 2006.

Hydrogen Production by Water Dissociation Using Mixed-Conducting Dense Ceramic Membranes, Intl. J. of Hydrogen Energy, 32, 451 (2007).

Reforming of Natural Gas via Water Splitting Using Dense Ceramic Membranes, presented at Natl. Hydrogen Assoc. Meeting, San Antonio, TX, March 19-22, 2007.

Hydrogen Production by Water Splitting Using Mixed Ionic-Electronic Conducting Membranes, presented at 211<sup>th</sup> Meeting of Electrochem. Soc., Chicago, IL, May 6-10, 2007.

Hydrogen Production by Reforming of Natural Gas via Water Splitting using Dense Ceramic Membranes, presented at Intl. Symposium on Materials Issues in a Hydrogen Economy, Richmond, VA, Nov. 12-15, 2007.

Hydrogen Production by Water Dissociation Using Oxygen Transport Membranes, presented at 213<sup>th</sup> Electrochemical Soc. Meeting, May 18-23, 2008, Phoenix, Arizona.

$\text{La}_{0.7}\text{Sr}_{0.3}\text{Cu}_{0.2}\text{Fe}_{0.8}\text{O}_{3-x}$  as Oxygen Transport Membrane for Producing Hydrogen via Water Splitting, presented at 213<sup>th</sup> Electrochemical Soc. Meeting, Phoenix, Arizona, May 18-23, 2008.

## REFERENCES

- [1] U. Balachandran et al., Argonne National Laboratory Hydrogen Separation Membranes--Annual Report for FY 2003.
- [2] U. Balachandran et al., Argonne National Laboratory Hydrogen Separation Membranes--Annual Report for FY 2002.
- [3] S. Ihara, Bull. Electrotech. Lab., 41, 259-280 (1977).
- [4] B. Ma, et al., Ceram. Trans., 73, 169-177 (1997).
- [5] P. S. Maiya, et al., Solid State Ionics, 99, 1-7 (1997).
- [6] L. Qiu, et al., Solid State Ionics, 76, 321-329 (1995).
- [7] T. H. Lee, et al., Solid State Ionics, 100, 77-85 (1997).
- [8] H. Naito and H. Arashi, Solid State Ionics, 79, 366-370 (1995).
- [9] U. Balachandran et al., Hydrogen Separation Membranes--Annual Report for FY 2000, Argonne National Laboratory.
- [10] J.R. Jurado, F.M. Figueiredo, B. Gharbage, and J.R. Frade, Solid State Ionics, 118, 89 (1999).
- [11] U. Balachandran et al., Hydrogen Production by Water Dissociation Using Ceramic Membranes--Annual Report for FY 2007, Argonne National Laboratory.
- [12] U. Balachandran et al., Hydrogen Production by Water Dissociation Using Ceramic Membranes--Annual Report for FY 2004, Argonne National Laboratory.



**Energy Systems Division**

Argonne National Laboratory  
9700 South Cass Avenue, Bldg. 212  
Argonne, IL 60439-4838

[www.anl.gov](http://www.anl.gov)



U.S. DEPARTMENT OF  
**ENERGY**

A U.S. Department of Energy laboratory  
managed by UChicago Argonne, LLC